Journal of Materials Chemistry C

Accepted Manuscript

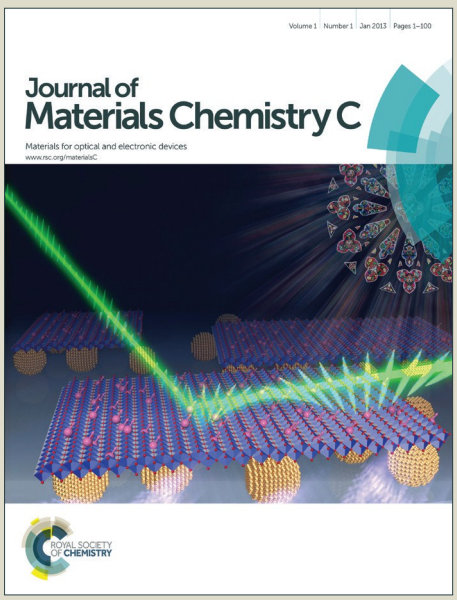

ROYAL SOCIETY OF CHEMISTRY

www.rsc.org/materialsC

Journal of Materials Chemistry C

COMMUNICATION

Light-Blue Thermally Activated Delayed Fluorescent Emitters Realizing a High External Quantum Efficiency of 25% and Unprecedented Low Drive Voltages in OLEDs

Received 00th January 20xx,
Accepted 00th January 20xx

DOI: 10.1039/x0xx00000x

www.rsc.org/

Ryutaro Komatsu,[a] Hisahiro Sasabe,*[a,b] Yuki Seino,[a] Kohei Nakao,[a] and Junji Kido*[a,b]

Thermally activated delayed fluorescent (TADF) emitters are one of the most promising candidates for low-cost and high efficiency organic light-emitting devices (OLEDs) to realize an internal quantum efficiency of unity. However, the power efficiency (η_p), which is inversely related to drive voltage, is significantly lower than that of the phosphorescent counterparts, especially for blue devices. Here, we developed a series of TADF emitters, 2-functionalized-4,6-bis[4-(9,9-dimethyl-9,10-dihydroacridine)phenyl]pyrimidine called Ac–RPM. We introduced a phenylacridine moiety into the 4,6-position of pyrimidine core to induce a twisted structure leading to a high photoluminescent quantum yield of ~80%, and a small singlet and triplet excited energy difference of <0.20 eV. The optimized device realized an η_p of 62 lm W^{-1}, a high external quantum efficiency of 25%, light-blue emissions with the Commission Internationale de l'Eclairage chromaticity coordinates of (0.19, 0.37) and a low turn-on voltage of <3.0 V.

Highly efficient organic light-emitting devices (OLEDs) are one of the most promising green technologies for future lighting and flat-panel display applications. [1–8] Unlike conventional light sources, OLEDs have outstanding advantages, such as area lighting, because they are ultra-thin, lightweight, and flexible when a flexible substrate is used. Until very recently, phosphorescent emitters containing platinum heavy metals, such as Ir, Os, and Pt, were required for high-performance OLEDs to realize 100% internal quantum efficiencies (IQE) because these platinum heavy metals can harvest all the electrogenerated molecular excitons. Phosphorescent OLEDs have already achieved a high external quantum efficiency (η_{ext}) of >30% and low drive voltages for the three primary colors, leading to high power efficiencies (η_p).[9–15]

Recently, thermally activated delayed fluorescent (TADF) emitters consisting of pure organic compounds have been considered as an alternate technology to harvest all the molecular excitons without the use of expensive platinum group metals and are thus able to realize an IQE of 100%.[16] Indeed, several green TADF devices have achieved a high η_{ext} of 30% and/or high η_p of ~90 lm W^{-1}.[17, 18] However, the corresponding blue TADF devices still require development to reach the η_p levels of state-of-the-art blue phosphorescent devices. Recently, a few highly efficient blue TADF devices with η_{ext} of over 20% have been reported.[19–24] Adachi and co-workers developed bis[4-(9,9-dimethyl-9,10-dihydroacridine)phenyl]sulfone composed of two acridine (Ac) moieties as donors and one diphenylsulfone moiety as an acceptor.[19] The same group developed a carbazole/triazine-based light-blue TADF emitter exbihiting a high η_{ext} of 20% with a relatively low turn-on voltage (V_{on}) of 4.0 V.[20] More recently, Lee and co-workers developed a light-blue TADF emitter, TCzTrz, composed of one triphenyltriazine moiety and three carbazole moieties showing a maximum external quantum efficiency ($\eta_{ext,max}$) of 25% and a maximum power efficiencies of ($\eta_{p,max}$) of 43 lm W^{-1} with a V_{on} of 4.0 V.[23] As mentioned above, blue TADF devices have not reached the efficiency levels of state-of-the-art blue

[a] Department of Organic Device Engineering, Graduate School of Science and Engineering, Yamagata University, Yonezawa, Yamagata, 992-8510 Japan.
[b] Research Center for Organic Electronics (ROEL), Yamagata University, Yonezawa, Yamagata, 992-8510 Japan.
This study was partially supported by KAKENHI Grant Numbers (26620202) and (25-7551).

phosphorescent devices; however, they should be able to achieve a high η_p without any loss of η_{ext}.

In this report, we developed a novel series of TADF emitters, 2-functionalized-4,6-bis[4-(9,9-dimethyl-9,10-dihydroacridine)phenyl]pyrimidine called **Ac–RPM** composed of one pyrimidine (PM) and two Ac moieties. This series of **Ac–RPM** derivatives exhibited a high photoluminescent quantum yield (η_{PL}) of 77%–80% and delayed fluorescence lifetime (τ_d) of 21–26 μs in a solid host matrix. The optimized OLED showed light-blue emissions with Commission Internationale de l'Eclairage (CIE) chromaticity coordinates of (0.19, 0.37), and realized a high $\eta_{p,max}$ of 62 lm W^{-1}, a high $\eta_{ext,max}$ of 25%, and an unprecedentedly low V_{on} of 2.8 V, which is the lowest V_{on} to date.

Although conventional fluorescent blue emitters composed of PM and donor moieties, such as alkyl amines, carbazoles, and thiophenes, are well known throughout the past decade as efficient fluorescent emitters with high η_{PL} values, the PM moiety has not been used as a component of TADF emitters. [25, 26] A large variety of TADF emitters could be developed using PM because the 2,4,6-positions of the PM moiety is easily functionalized. In the development of TADF emitters, the energy difference between the singlet and triplet excited states (ΔE_{ST}) must be small (<0.2 eV) to obtain the TADF character.[20] For this, a twisting π-conjugated system between the donor and accepter moieties in the molecule is a promising design strategy. Here, for the donor, we introduced a phenylacridine moiety into the 4,6-position of the PM moiety to induce a twisted structure in the molecule. Three different **Ac–RPM** derivatives (**Ac–HPM**, **Ac–PPM**, and **Ac–MPM**, where R = H, phenyl, and CH_3, respectively) were introduced at the 2-position of PM (**Figure 1**).

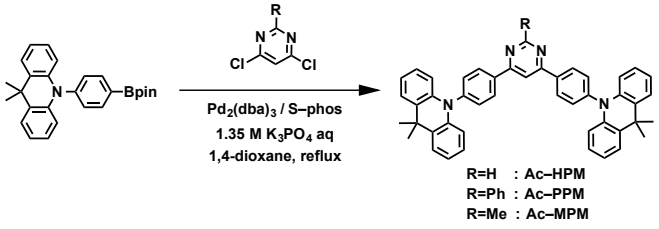

Figure 1. Synthetic routes and chemical structures of **Ac–RPM** derivatives.

Prior to the preparation of the materials, we conducted density functional theory calculations to estimate their geometrical structures, ΔE_{ST}, and energy gap (E_g) of the **Ac–RPM** (**Figure S-1, Figure 2** and **Table S-1**). All **Ac–RPM** derivatives showed a very small ΔE_{ST} of 0.01 eV and a wide energy gap of >3.3 eV; thus, a blue TADF emission was expected (**Table S-1**). The electron cloud distribution in **Figure 2** shows that the highest occupied molecular orbital (HOMO) is located on the Ac moiety, whereas the lowest unoccupied molecular orbital (LUMO) is located on the 4,6-diphenylpyrimidine skeleton. The frontier molecular orbitals, in other words, HOMO and LUMO, are almost completely separated, with a very-small overlap.

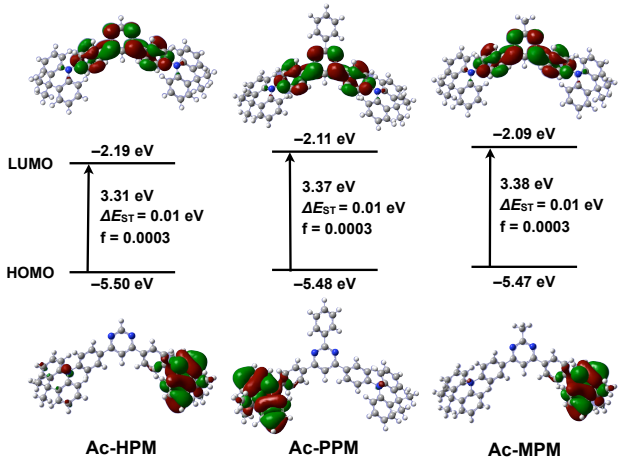

Figure 2. HOMO and LUMO distribution, energy levels, optical energy gap (E_g), the energy difference between the singlet and triplet excited states (ΔE_{ST}), and oscillator strength (f) of **Ac–RPM** derivatives.

The synthetic routes of **Ac–RPM** are shown in **Figure 1**. The precursor boronate ester, Ac–Bpin, can be easily prepared according to the literature.[27] A Suzuki–Miyaura coupling reaction of Ac–Bpin with 2-functionalized-4,6-dichloropyrimidine afforded **Ac–RPM** in a reasonable yield. This simple, one-step synthesis allows a large amount of **Ac–RPM** to be prepared on a multigram scale. Characterization was performed using ^{1}H-NMR, mass spectroscopy, and elemental analysis. The product was purified by train sublimation before device fabrication.

The thermal properties were estimated by thermogravimetric analysis (TGA) and differential scanning calorimetry (DSC) (**Figure S-2**). A weight loss of 5% (T_{d5}) was observed at temperatures over 430 ˚C, which indicates high thermal stability and is applicable for thermal evaporation, whereas a glass-transition temperature was not observed between 50 °C and 380 °C.

Table 1. Thermal and photophysical properties of **Ac–RPM** derivatives.

Compound	$T_g/T_m/T_{d5}$ [°C][a]	$I_p/E_a/E_g$ [eV][b]	$E_S/E_T/\Delta E_{ST}$ [eV][c]	τ_d [μs][d]	η_{PL} [%][e]
Ac–HPM	n.d./325/430	5.65/2.84/2.81	2.84/2.66/0.18	21.4	77
Ac–PPM	n.d./388/442	5.65/2.85/2.80	2.84/2.65/0.19	20.7	79
Ac–MPM	n.d./348/432	5.66/2.85/2.81	2.89/2.70/0.19	26.2	80

[a] T_g and T_m were measured by DSC; T_{d5} was measured by TGA. [b] I_p was measured by PYS; The E_g was taken as the point of intersection of the normalized absorption spectra; E_a was calculated by using I_p and E_g. [c] Onset of phosphorescence of 10 wt% **Ac–RPM**-doped DPEPO film were measured by using a streak camera. $\Delta E_{ST} = E_S - E_T$. [d] Delayed fluorescent lifetime of 10 wt% **Ac–RPM**-doped DPEPO film. [e] Photoluminescent quantum yield of 10 wt% **Ac–RPM**-doped DPEPO film.

The optical properties were evaluated in dilute toluene solution. The ultraviolet-visible (UV-vis) absorption and photoluminescent (PL) spectroscopy spectra of **Ac–RPM** measured at room temperature are shown in **Figure 3**. The weak absorption of approximately 380 nm can be attributed to the intramolecular charge transfer state from the Ac moiety to the PM moiety. The absorption coefficient was calculated as approximately 4.0×10^3 M^{-1} cm^{-1}. The emission peaks of **Ac–HPM**, **Ac–PPM**, and **Ac–MPM** are very similar, located at 489, 484, and 478 nm, respectively (**Table S-2**). These emission peaks are well consistent with the results of E_g estimated by DFT calculation. The electron-donating property of methyl group makes the LUMO level shallower thus leading to wider E_g of **Ac–MPM**. **Ac–RPM** derivatives show light-blue emissions in dilute toluene solution. The physical properties of the material were evaluated in the solid state. The ionization potential (I_p) levels, which were measured by photoelectron yield spectroscopy (PYS), were observed at approximately 5.7 eV. The electron affinity (E_a) levels were estimated at approximately 2.9 eV by the subtraction of the optical energy gap (E_g) from the I_p levels.

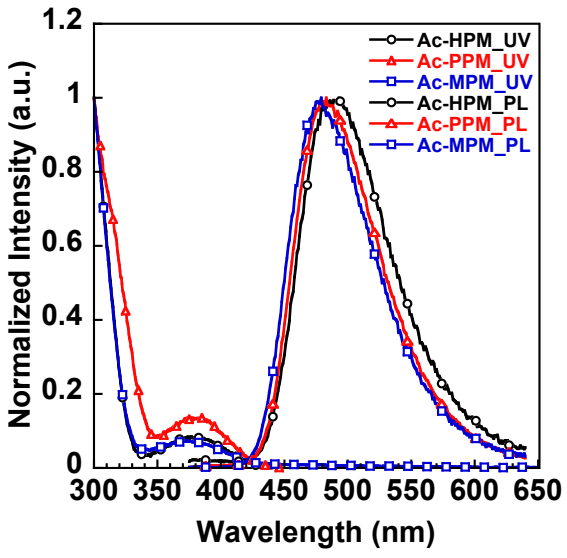

Figure 3. UV–vis and PL spectra of **Ac–RPM** in toluene (1.0×10^{-5} M).

The PL spectra were then investigated in a host matrix of bis[2–(diphenylphosphino) phenyl]ether oxide (DPEPO)[19], which has high triple energy (E_T). As shown in **Figure S-3**, the emission peaks of 10 wt% **Ac–HPM**-, **Ac–PPM**-, and **Ac–MPM**-doped DPEPO films are located at 498, 498, and 489 nm, respectively. The emission peaks of these films show an approximate 10-nm red shift compared with the solution states.

The η_{PL} values of the Ac–RPM derivatives were then evaluated. The η_{PLs} of the 10 wt% **Ac–RPM**-doped DPEPO films were measured under N_2 flow using an integrating sphere with an excitation light at 290 nm, with a multichannel spectrometer as the optical detector. The η_{PL} values of 10 wt% **Ac–HPM**-, **Ac–PPM**-, and **Ac–MPM**-doped DPEPO films are 77%, 79%, and 80%, respectively. The TADF character is confirmed by the means of the transient PL decay curve at a high temperature of 300 K (**Figure 4**). The delayed PL intensities of the three materials increase at 300 K, which indicates the presence of TADF. Transient PL decay curves of 10 wt% **Ac–RPM**-doped DPEPO films exhibit a triple-exponential decay with a delayed lifetime (τ_d) of 21–26 μs. ΔE_{ST} was estimated from the onset of the prompt and delayed emission components to be approximately 0.20 eV at 5 K (**Figure S-4**). All photophysical properties of **Ac–RPM** derivatives are summerized in **Table 1**.

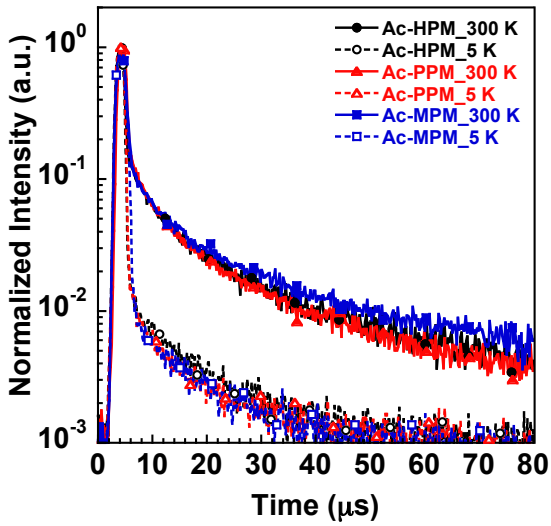

Figure 4. Transient PL decay curves of **Ac–RPM** at 5 K and 300 K.

Next, we evaluated OLED performances. In our TADF devices, we used a carrier- and exciton-confining device structure to maximize the OLED performance. We used di-[4-(N,N-ditolyl-amino)-phenyl]cyclohexane (TAPC) as a hole transport layer (HTL), DPEPO as a host material, and 3,3'',5,5'-tetra(3-pyridyl)-1,1';3',1''-terphenyl (B3PyPB)[28] as an electron transport layer (ETL). The triplet energy (E_T) levels of TAPC, DPEPO, and B3PyPB are 2.98, 3.30, and 2.77 eV, respectively. All the materials have a higher E_T than that of **Ac–RPM** derivatives (E_T = 2.65–2.67 eV). Therefore, the triplet excitons of the emitter can be completely suppressed. All the chemical structures of materials used in this study are shown in **Figure S-5**. Three types of OLEDs with a structure of [ITO/TAPC (30 nm)/10 wt% **Ac–RPM**:DPEPO (20 nm) /B3PyPB (50 nm)/LiF (0.5 nm)/Al (100 nm)] were fabricated. **Figure S-6a** shows the energy diagrams of these devices. All the EL spectra show an emission only from **Ac–RPM** with no emission from neighboring materials. The CIE chromaticity coordinates (x, y) for **Ac–HPM** and **Ac–PPM** were evaluated as (0.21, 0.44), which is located in the green emission region, whereas the Ac–MPM-based device shows a light-blue emission with the CIE coordinates of (0.19, 0.37). All the devices show very-high η_{ext} of approximately 20% and η_p of over 50 lm W^{-1} with an unprecedented V_{on} of 2.9 V (**Figure S-7** and **Table 2**) To obtain a better understanding of the operation mechanism in the **Ac-MPM**-based device, we compared three types of devices with emission layers (EMLs) of (A) 10 wt% **Ac–MPM**-doped DPEPO (20 nm); (B) 10 wt% **Ac–MPM**-doped DPEPO (10 nm)/ DPEPO (10 nm); and (C) DPEPO (10 nm)/ 10 wt% **Ac–MPM**-doped DPEPO (10 nm). **Figure S-8** shows the energy diagrams of these devices, and all the device performances are summarized in **Table S-3**. The EL spectra of devices (A) and (B) are the same and show emissions from only **Ac–MPM** (**Figure S-9**), whereas the spectrum of device (C) shows an emission from **Ac–MPM** along with an emission at λ_{max} = 580 nm, which is identical to the emission from the electromer of TAPC.[29] Devices (A) and (B) show similar *J–V* characteristics (**Figure S-9**), indicating that their carrier recombination pathways are similar, whereas device (C) is completely different, probably because of the poor hole injection ability of DPEPO. Thus, it can be considered that the carrier recombination zone is located near the HTL/EML interface.

Table 2. Summary of OLED performances.

Emitter	Host	V_{on}/ $\eta_{p,\,on}$/$\eta_{c,\,on}$/$\eta_{ext,\,on}$ [V/ lm W^{-1}/ cd A^{-1}/ %][a]	V_{100}/ $\eta_{p,\,100}$/$\eta_{c,\,100}$/$\eta_{ext,\,100}$ [V/ lm W^{-1}/ cd A^{-1}/ %][b]	V_{1000}/$\eta_{p,\,1000}$/$\eta_{c,\,1000}$/$\eta_{ext,\,1000}$ [V/ lm W^{-1}/ cd A^{-1}/ %][c]	CIE (x, y)[d]
Ac–HPM	DPEPO	2.85 / 60.3 / 54.7 / 20.9	3.79 / 38.2 / 46.0 / 17.6	4.82 / 20.0 / 30.6 / 11.7	(0.21, 0.44)
Ac–PPM	DPEPO	2.93 / 52.8 / 49.2 / 19.0	4.01 / 33.8 / 43.2 / 16.6	5.25 / 17.4 / 29.0 / 11.2	(0.21, 0.44)
Ac–MPM	DPEPO	2.93 / 49.9 / 46.6 / 20.4	3.96 / 29.2 / 36.8 / 16.1	5.27 / 13.2 / 22.1 / 9.7	(0.19, 0.37)
Ac–MPM	mCP/DPEPO	2.80 / 61.6 / 54.9 / 24.5	3.57 / 34.0 / 38.5 / 17.2	4.57 / 15.5 / 22.5 / 10.1	(0.19, 0.37)

[a] Voltge (V), power efficiency (η_p), current efficiency (η_c) and external quantum efficiency (η_{ext}) at 1 cd m^{-2}. [b] V, η_p, η_c, and η_{ext} at 100 cd m^{-2}. [c] V, η_p, η_c, and η_{ext} at 1000 cd m^{-2}. [d] CIE at 100 cd m^{-2}.

Considering the above results, there is still much room to improve the carrier balance in the EML by introducing a hole transporting material that is superior to DPEPO between the HTL and the EML. Therefore, we introduced N,N-dicarbazoyl-3,5-benzene (mCP) with a shallower I_p level (6.0 eV) than that of DPEPO (6.7 eV). In other words, we used a double emission layer (DEML) strategy using mCP/DPEPO host materials. We fabricated a DEML device with a structure of [ITO/TAPC (30 nm)/10 wt% **Ac–MPM**-doped mCP (10 nm)/10 wt% **Ac–MPM**-doped DPEPO (10 nm) /B3PyPB (50 nm)/ LiF (0.5 nm)/Al (100 nm)]. **Figure S-6b** shows the energy diagrams of these devices. The *J–V–L* and the *PE–L–EQE* characteristics are shown in **Figure 5**. This light-blue device with λ_{EL} = 487 nm achieves an $\eta_{ext,max}$ of 24.5% and $\eta_{p,max}$ of 61.6 lm W^{-1} with a low V_{on} of 2.80 V. The V_{on} is very close to the energy-gap-voltage values of **Ac–MPM** (2.54 eV). Even at 100 cd m^{-2}, a $\eta_{ext,100}$ of 17.2%, $\eta_{p,100}$ of 34 lm W^{-1}, and V_{100} of 3.57 V are realized.

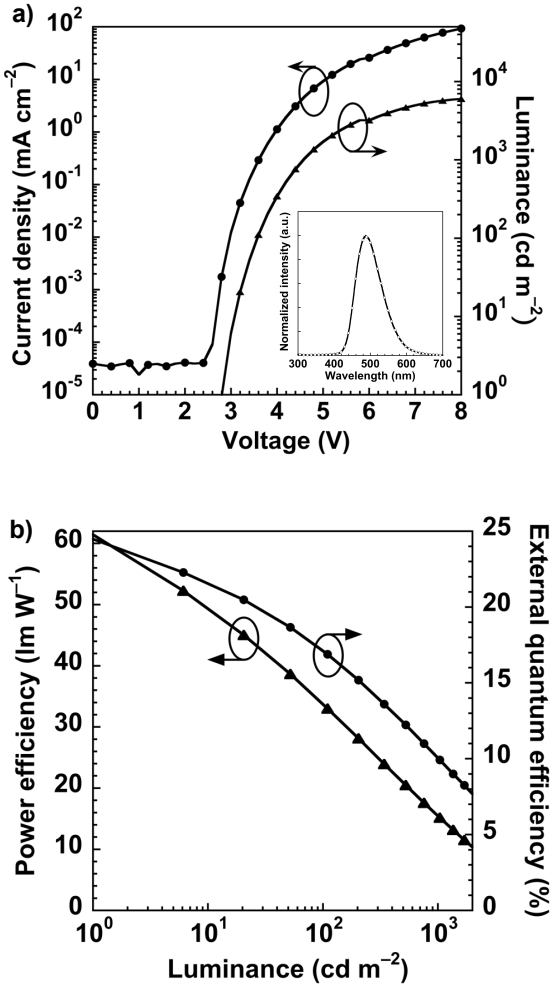

Figure 5. a) *J–V–L* characteristics, inset: EL spectra at 0.5 mA, and b) *PE–EQE–L* characteristics of **Ac–MPM**-based OLEDs.

In summary, we have developed a novel series of TADF emitters called **Ac–RPM** derivatives using a PM/Ac combination. These derivatives exhibited a light-blue emission in a toluene solution. Among these, **Ac–MPM** showed an intense emission with a high η_{PL} of 80%, and a τ_d of 26 μs in a DPEPO host matrix. By a carrier- and exciton-confining structure, the optimized OLED showed a light-blue emission and realized a high $\eta_{p,max}$ of 62 lm W^{-1} and a high $\eta_{ext,max}$ of 25% with an unprecedentedly low V_{on} of 2.8 V, which is the lowest V_{on} so far (**Table S-4**).[19–24] For the practical application of blue TADF devices, there are still several challenges, such as pure-blue emission, reduced efficiency roll-off at high current density, and low drive voltage at high brightness. Further design and synthesis of novel blue TADF emitters are currently being developed in our laboratory. We believe that our results can accelerate the development of TADF OLED technology for future lighting applications.

[1] J. Kido, M. Kimura, K. Nagai, *Science*, 1995, **267**, 1332–1334.

[2] Y. Sun, N. C. Giebink, H. Kanno, B. Ma, M. E. Thompson, S. R. Forrest, *Nature*, 2006, **440**, 908–912.

[3] B. W. D'Andrade, J. Esler, C. Lin, V. Adamovich, S. Xia, M. S. Weaver, R. Kwong, J. J. Brown, *Proc. SPIE*, 2008, **7051**, 70510Q-1.

[4] S. Reineke, F. Lindner, G. Schwartz, N. Seidler, K. Walzer, B. Lussem, K. Leo, *Nature*, 2009, **459**, 234–238.

[5] M. G. Helander, Z. B. Wang, J. Qiu, M. T. Greiner, D. P. Puzzo, Z. W. Liu, Z. H. Lu, *Science*, 2011, **332**, 944–947.

[6] T.-H. Han, Y. Lee, M.-R Choi, S.-H. Woo, S.-H. Bae, B. H. Hong, J.-H. Ahn & T.-W. Lee, *Nat. Photon.*, 2012, **6**, 105–110.

[7] H. Sasabe, J. Kido, *J. Mater. Chem. C*, 2013, **1**, 1699–1707.

[8] H. Sasabe, J. Kido, *Eur. J. Org. Chem.*, 2013, 7653–7663.

[9] D. Tanaka, H. Sasabe, Y.-J. Li, S.-J. Su, T. Takeda, J. Kido, Jpn. *J. Appl. Phys.*, 2007, **46**, L10–L12.

[10] C. W. Lee, J. Y. Lee, *Adv. Mater.*, 2013, **25**, 5450–5454.

[11] J.-H. Lee, S.-H. Cheng, S.-J. Yoo, H. Shin, J.-H. Chang, C.-I. Wu, K.-T. Wong, J.-J. Kim, *Adv. Funct. Mater.*, 2015, **25**, 361–366.

[12] K.-H. Kim, S. Lee, C.-K. Moon, S.-Y. Kim, Y.-S. Park, J.-H. Lee, J. W. Lee, J. Huh, Y. You, J.-J. Kim, *Nat. Commun.*, 2014, **5**, 4769.

[13] H. Sasabe, H. Nakanishi Y. Watanabe, S. Yano, M. Hirasawa, Y.-J. Pu, J. Kido, *Adv. Funct. Mater.*, 2013, **23**, 5550–5555.

[14] K. Udagawa, H. Sasabe, C. Cai, J. Kido, *Adv. Mater.*, 2015, **26**, 5062–5066.

[15] K. Udagawa, H. Sasabe, F. Igarashi, J. Kido, *Adv. Opt. Mater.*, DOI: 10.1002/adom.201500462.

[16] H. Uoyama, K. Goushi, K. Shizu, H. Nomura, C. Adachi, *Nature*, 2012, **492**, 234–238.

[17] J. W. Sun, J.-H. Lee, C.-K. Moon, K.-H. Kim, H. Shin, J.-J. Kim, *Adv. Mater.*, 2014, **26**, 5684–5688.

[18] D. R. Lee, B. S. Kim, C. W. Lee, Y. Im, K. S. Yook, S.-H. Hwang, J. Y. Lee, *ACS Appl. Mater. Interf.*, 2015, **7**, 9625–9629.

[19] Q. Zhang, B. Li, S. P. Huang, H. Nomura, H. Tanaka, C. Adachi, *Nat. Photon.*, 2014, **8**, 326–332.

[20] S. Hirata, Y. Sakai, K. Masui, H. Tanaka, S. Y. Lee, H. Nomura, N. Nakamura, M. Yasumatsu, H. Nakanotani, Q. Zhang, K. Shizu, H. Miyazaki, C. Adachi, *Nat. Mater.*, 2015, **14**, 330–336.

[21] M. Numata, T. Yasuda, C. Adachi, *Chem. Commun.*, 2015, **51**, 9443–9446.

[22] W. Liu, C.-J. Zheng, K. Wang, Z. Chen, D.-Y. Chen, F. Li, X.-M. Ou, Y.-P. Dong, X.-H. Zhang, *ACS Appl. Mater. Interf.*, 2015, **7**, 18930–18936.

[23] D. Y. Lee, M. Kim, S. K. Jeon, S.-H. Hwang, C. W. Lee, J. Y. Lee, *Adv. Mater.*, 2015, **27**, 5861–5867.

[24] J. W. Sun, J. Y. Beak, K.-H. Kim, C.-K. Moon, J.-H. Lee, S.-K. Kwon, Y.-H. Kim, and J.-J. Kim, *Chem. Mater.*, 2015, **27**, 6675–6681.

[25] S. Kato, Y. Yamada, H. Hiyoshi, K. Umezu, Y. Nakamura, *J. Org. Chem.*, 2015, **80**, 8356–8359.

[26] S. Achelle, N. Pie, *Curr. Org. Synth.*, 2012, **9**, 163–216.

[27] S. Y. Lee, T. Yasuda, I. S. Park, C. Adachi, *Dalton Trans.*, 2015, **44**, 8356–8359.

[28] H. Sasabe, E. Gonmori, T. Chiba, Y.-J. Li, D. Tanaka, S.-J. Su, T. Takeda, Y.-J. Pu, K. Nakayama, J. Kido, *Chem. Mater.*, 2008, 20, 5951–5953.

[29] J. Kalinowski, G. Giro, M. Cocchi, V. Fattori, P. D. Marco, *Appl. Phys. Lett.* 2000, **76**, 2352–2354.

Graphical abstract

Light-Blue Thermally Activated Delayed Fluorescent Emitters Realizing a High External Quantum Efficiency of 25% and Unprecedented Low Drive Voltages in OLEDs

By Ryutaro Komatsu, Hisahiro Sasabe*, Yuki Seino, Kohei Nakao, and Junji Kido*

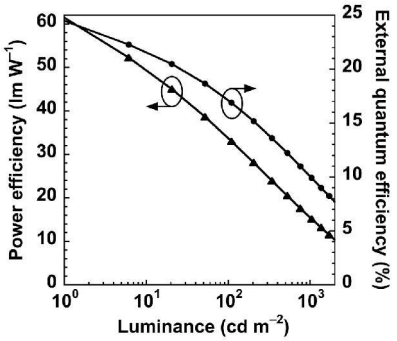

A series of thermally activated delayed fluorescent (TADF) emitters called **Ac–RPM**, composed of one pyrimidine and two acridine moieties are developed. The optimized device realized its highest power efficiency of 62 lm W^{-1}, a high external quantum efficiency of 25%, light-blue emissions with the Commission Internationale de l'Eclairage chromaticity coordinates of (0.19, 0.37) and an unprecedentedly low turn-on voltage of <3.0 V.